Simulation and Analysis of Core Losses Under High-Frequency PWM Wave Voltage Excitations

Zhikang FU, Jinghui WANG, Juntao XIAO, and Wei CHEN

Abstract—**The core losses quantification of magnetic components with geometrically diverse cores for power converters remains a challenge and an area of active research. By using finite element analysis software Ansys Maxwell, a simulation method for core losses calculation under PWM voltage excitation is proposed based on the modified Steinmetz equation (MSE) in this paper. The magnetic properties measurement and model of core material are specified, which are basis of core losses simulation. Furthermore, the work conducts a comprehensive error analysis to identify primary sources of simulation inaccuracies, accompanied by targeted mitigation strategies. To validate the methodology, core losses of a ferrite EE shaped core are simulated and subsequently compared with experimental measurements acquired through the DC power method. The close agreement between simulated and empirical results demonstrates the efficacy of the proposed methodology.**

Index Terms—**Core loss model, core losses simulation, DC power method, finite element analysis, PWM wave excitation.**

I. Introduction

MAGNETIC components are important passive component in power converters, and their losses are important indicators for the optimal design of power converters. The losses of magnetic component include winding loss and core losses. The winding loss which is of a linear nature can be accurately obtained by using an impedance analyzer or finite element software when the winding's material is solid conductor. However, the accurate quantification of Litz wire winding losses remains a difficult problem [1]–[2]. The core losses are of a nonlinear nature and are affected by numerous factors. Not only do the excitation voltage waveform, frequency, amplitude, as well as the working environment and temperature affect the core losses, but also the core material, core shape and size have an impact on the core losses. As the frequency, efficiency and power density of power converters are getting higher and higher [3]–[4], the shapes of cores are becoming more and more diverse. The error will be very large if we only use the mathematical model of core losses to predict the core losses of cores with various shapes. Although the losses of magnetic components can be obtained through measurement, it is extremely unrealistic and uneconomical to measure the losses of each designed product after prototyping to verify whether it meets the design requirements [5]–[6].

Finite element analysis (FEA) is a numerical analysis method for analyzing the magnetic flux density distribution of irregular cores. In the industry, it tends to be used to obtain the core losses of magnetic components with different core shapes. Ansys Maxwell is the most commonly used FEA simulation software in the industry. Based on the accurate calculation of the magnetic flux density distribution within the core, the core losses prediction models which come with software are utilized to obtain the core losses of magnetic components. There are three types of core losses prediction models built into the software: the Steinmetz equation (SE) model, the loss separation model and the P_{cv}-B_m curve. The SE model is only applicable to the core losses calculation under sinusoidal excitation. Based on the core losses under sinusoidal excitation, the loss separation model divides the core losses into hysteresis loss, classical eddy current loss and excess eddy loss according to the physical mechanism of core losses[7], [8]–[9] proposed an improved loss separation model, and extended it to core losses calculation under non-sinusoidal excitation. The P_{cv}-B_m curve is directly the numerical relationship between the core losses density P_{cv} and the peak value of the magnetic flux density B_m. However, the P_{cv}-B_m relationship curves for different excitation frequencies are different, so it is only applicable to the core losses simulation at a single frequency. Finite element (FE) software is used to obtain the core losses of cores with different structures, which is beneficial to enterprises to reducing research and development costs. However, the core losses simulation methods of existing software are not applicable to core losses calculation of magnetic components in power converters.

Accurate core losses measurement is the basis of core losses simulation and also the means of verifying the core losses simulation accuracy. The existing core losses measurement methods are mainly divided into non-electrical methods and electrical methods. Calorimeter method is recognized as the most accurate non-electrical measurement method for core losses. However, it is complicated to operate, time-consuming

Manuscript received January 04, 2025; revised February 19, 2025; accepted March 14, 2025. Date of publication June 30, 2025; date of current version April 18, 2025. This work was supported in part by National Natural Science Foundation of China under the grant 51777036. *(Corresponding author: Jinghui Wang.)*

Z. Fu, J. Wang, and W. Chen are with the College of Electrical Engineering and Automation, Fuzhou University, Fuzhou 350108, China (e-mail: 417423447@qq.com; wjh@fzu.edu.cn; chw@fzu.edu.cn).

J. Xiao is with the Delta Electronics Shanghai Co., Ltd., Shanghai 201209, China (e-mail: 645138025@qq.com).

Digital Object Identifier 10.24295/CPSSTPEA.2025.00014

and has strict environmental requirements [10]–[11]. Electrical methods mainly include the Two-Winding AC power method and the DC power method. Regarding the Two-Winding AC power method, the voltage on the sensing winding and the current on the excitation winding of the magnetic component are sampled, and the core losses can be obtained by calculating the average value of the product of the two. When the impedance angle of the tested component is close to 90°, a tiny phase-difference error will lead to a very large measurement error [12]–[13]. [13] utilizes reactive power compensation to reduce the phase difference between the sampled voltage and current so as to improve the measurement accuracy of the Two-Winding AC power method. Regarding the DC power method, an inverter circuit is used to convert the DC voltage into a high-frequency PWM wave and apply it to the magnetic component. The output power of the DC voltage is measured to obtain the losses of the magnetic component, which effectively circumvents the problem that the measurement error of the Two-Winding AC power method is sensitive to the phase difference error. The loss of the inverter circuit is the main error source of the DC power method. An air-core inductor is used for calibration to verify the losses of the inverter circuit so as to improve the measurement accuracy of the DC power method [14]. The differential DC power method is proposed to broaden the inductance range of the tested components based on the DC power method [15].

In this paper, based on the modified Steinmetz equation (MSE), a simulation scheme for the core losses of magnetic components under high-frequency PWM wave voltage excitation by using the FE software Ansys Maxwell is proposed. The sources of calculation errors are analyzed in detail and corresponding solutions are put forward. Finally, based on the accurate measurement and models of the magnetic properties of core materials, the core losses of EE-shaped cores made of the same material are simulated and analyzed by utilizing the proposed simulation scheme. The simulation results are compared with the measured values of core losses to verify the feasibility and accuracy of the simulation scheme.

II. Simulation Scheme for Core Losses under High-Frequency PWM Wave Excitation

There are two key factors in the core losses calculation of magnetic components using the FE software Ansys Maxwell: 1) The mathematical prediction model of core losses density and magnetic flux density. The core losses are closely related to magnetic flux density, and an accurate mathematical model of core losses density is a guarantee for the core losses simulation of magnetic components. 2) The determination of the magnetic-flux-density distribution inside the core. FEA is to solve the Poisson equation or Laplace equation with known field-domain boundary conditions to obtain the magnetic vector potential. The curl of the magnetic vector potential is the magnetic-flux density. Among them, the permeability of the core-material is essential. Therefore, the accurate acquisition of the magnetization characteristics of the core material is the basis for the FE simulation of core losses.

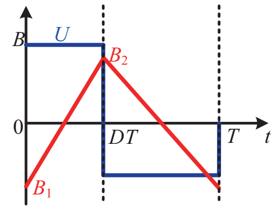

Fig. 1. Flux density waveform under PWM voltage excitation.

A. High-Frequency PWM Core Losses Mathematical Model

The Steinmetz equation is often used for the core losses calculation of magnetic components under sinusoidal excitation. [16] proposed an MSE for the core losses calculation of magnetic components under arbitrary waveform excitation. The weighted average magnetic flux density change rate B_{w} is introduced, as shown in (1).

$$B_{\mathrm{w}}=\frac{1}{2B_{\mathrm{m}}}\int_T\left(\frac{\mathrm{d}B}{\mathrm{d}t}\right)^2\mathrm{d}t \tag{1}$$

The equivalent sinusoidal wave frequency $f_{\mathrm{sin\_eq}}$ of an arbitrary waveform is obtained according to the equality of B_{w} for arbitrary-waveform excitation and sinusoidal-waveform excitation, as shown in (2).

$$f_{\mathrm{sin\_eq}}=\frac{2}{\Delta B^2\cdot\pi^2}\cdot\int_T\left(\frac{\mathrm{d}B}{\mathrm{d}t}\right)^2\mathrm{d}t \tag{2}$$

The core losses density under arbitrary waveform excitation $P_{\mathrm{cv\_arb}}$ can be obtained by using the core losses density under sinusoidal waveform excitation with a frequency of $f_{\mathrm{sin\_eq}}$, as shown in (3).

$$P_{\mathrm{cv\_arb}}=(k\cdot f_{\mathrm{sin\_eq}}^{\alpha-1}\cdot B_{\mathrm{m}}^{\beta})\cdot f_{\mathrm{s}} \tag{3}$$

where B_{m} is the peak value of AC magnetic flux density, k, α, and β are SE parameters of $f_{\mathrm{sin\_eq}}$, ΔB is the peak-to-peak value of the magnetic flux density, f_{s} is the excitation frequency of the arbitrary waveform.

The voltage excitation waveform and the magnetic flux density waveform of the PWM wave with a duty cycle of D and a frequency of f_{s} are shown in Fig. 1, and the magnetic flux density $B(t)$ is shown in (4).

$$B(t)=\begin{cases}B_1+\dfrac{B_2-B_1}{D}\cdot f_{\mathrm{s}}\cdot t & 0\leqslant t\leqslant DT\\ B_2-\dfrac{B_2-B_1}{(1-D)}\cdot f_{\mathrm{s}}\cdot(t-DT) & DT\leqslant t\leqslant T\end{cases} \tag{4}$$

The core losses density $P_{\mathrm{cv\_PWM}}$ under PWM wave voltage excitation can be obtained by combining (2), (3) and (4), as shown in (5).

$$P_{\mathrm{cv\_PWM}}=\left(\frac{\pi^2\cdot D\cdot(1-D)}{2}\right)\cdot k\cdot f_{\mathrm{sin\_eq}}^{\alpha}\cdot B_{\mathrm{m}}^{\beta} \tag{5}$$

The sinusoidal wave voltage excitation with frequency f_s is applied to the magnetic component, and the SE is used for the core losses calculation. Then, the PWM wave voltage excitation with a frequency f_s is applied to the magnetic component, and the MSE is used for its core losses calculation. When the peak values of the magnetic flux densities of the two are equal, the ratio of the core losses densities P_{cv_PWM}/P_{cv_sin} is shown in (6).

$$\frac{P_{cv\_PWM}}{P_{cv\_sin}} = \frac{(k \cdot f_{sin\_eq}^{\alpha-1} \cdot B_m^{\beta}) \cdot f_s}{k \cdot f_s^{\alpha} \cdot B_m^{\beta}} = (\frac{f_{sin\_eq}}{f_s})^{\alpha-1} \tag{6}$$

where P_{cv_sin} is the core losses density under sinusoidal wave voltage excitation, as shown in (7).

$$P_{cv\_sin} = k \cdot f_s^{\alpha} \cdot B_m^{\beta} \tag{7}$$

Thus the core losses density P_{cv_PWM} under PWM wave voltage excitation is shown in (8).

$$\begin{cases} P_{cv\_PWM} = \gamma \cdot k \cdot f_s^{\alpha} \cdot B_m^{\beta} = \gamma \cdot P_{cv\_sin} \\ \gamma = (\dfrac{2}{\pi^2 D(1-D)})^{\alpha-1} \\ k' = (\dfrac{2}{\pi^2 D(1-D)})^{\alpha-1} \cdot k \end{cases} \tag{8}$$

It can be derived from (8) that the ratio of the core losses under PWM wave excitation to that under sinusoidal wave excitation is a coefficient related to the duty cycle and the coefficient α when the excitation frequency and the peak value of the magnetic flux density are equal. Therefore, based on the core losses under sinusoidal wave excitation, the core losses under PWM wave voltage excitation can be simulated and calculated by using the eddy current field solver or the transient field solver of Maxwell software.

B. Simulation Process for Core Losses under High-Frequency PWM Wave Excitation

The flow chart of simulation scheme for core losses under high-frequency PWM voltage excitation is shown in Fig. 2. After establishing the simulation physical model, the modified Steinmetz parameters k', α, β and, the AC magnetization curve are assigned to the core material, and the copper material is assigned to the winding. Either the transient field solver or the eddy current field solver can be selected.

If the transient field solver is chosen, the PWM wave voltage excitation is applied to the magnetic component, and the magnetic flux density distribution inside the core is obtained. The core losses density distribution inside the core is calculated by using the field calculator. Finally, the core losses of the magnetic component can be obtained by integrating the core losses density with the core volume.

If the eddy current field solver is chosen, the sinusoidal wave voltage excitation is applied to the magnetic component.

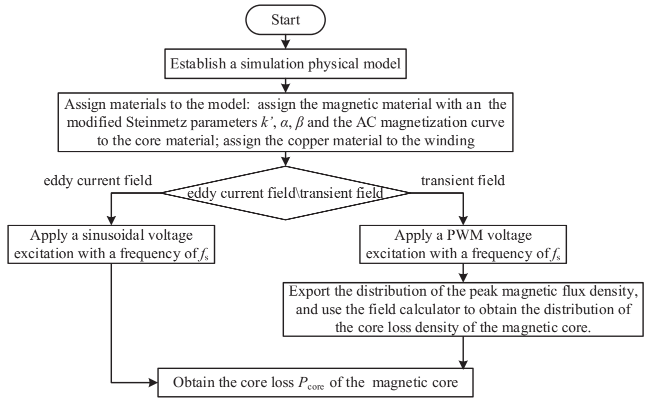

Fig. 2. Flow chart of core losses simulation for high-frequency PWM voltage excitation.

Then, the distribution of magnetic flux density peak inside the core can be directly obtained, and thus the core losses of magnetic components can be directly obtained. However, the sinusoidal wave voltage excitation can only be applied in the eddy current field solver. Therefore, it is necessary to determine the corresponding relationship between the sinusoidal-wave excitation voltage amplitude and the PWM excitation voltage amplitude, in order to ensure that the magnetic flux density amplitude of the two excitations is equal.

The relationships of the sinusoidal wave voltage amplitude U_{m_sin}, the peak-to-peak value of the PWM-wave voltage U_{pp_PWM} and the peak value of the magnetic flux density are shown in (9).

$$\begin{cases} U_{m\_sin} = 2 \cdot \pi \cdot f_s \cdot N \cdot A_e \cdot B_{m\_sin} \\ U_{pp\_PWM} = \dfrac{2 \cdot f_s \cdot N \cdot A_e}{D \cdot (1-D)} \cdot B_{m\_PWM} \end{cases} \tag{9}$$

If the core and winding turns of the magnetic component are the same, and the excitation frequency and the peak value of the magnetic flux density are also the same, the relationship between U_{m_sin} and U_{pp_PWM} is shown in (10).

$$\frac{U_{m\_sin}}{U_{pp\_PWM}} = \pi \cdot D \cdot (1-D) \tag{10}$$

C. Measurement of Magnetic Properties of Core Materials

As can be seen from Fig. 2, the accurate measurement of the magnetic properties of core material is the basis for the FE analysis and calculation of the core losses of magnetic components. This includes the measurement of the AC magnetization curve and the core losses under sinusoidal wave excitation.

In general, a magnetic ring with a relatively small ratio of outer diameter to inner diameter is used as the device under test (DUT) to obtain the magnetic properties of core material. In this paper, ferrite (TPG33B) is taken as the research object, and the ferrite T22 magnetic ring is employed to acquire the magnetic properties of core material. Its dimensional parameters are presented in Table I, and the effective

TABLE I
SIZE PARAMETERS OF FERRITE (TPG33B) T22 STANDARD MAGNETIC RING

parameter	value	parameter	value
OD (mm)	21.99	A_e (mm^2)	40.02
ID (mm)	14.05	V_e (mm^3)	2265.5
h (mm)	10.08	N (number of turns)	6
l_e (mm)	56	L (μH)	112.7

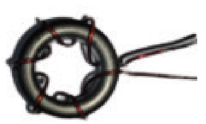

Fig. 3. Ferrite (TPG33B) T22 magnetic ring.

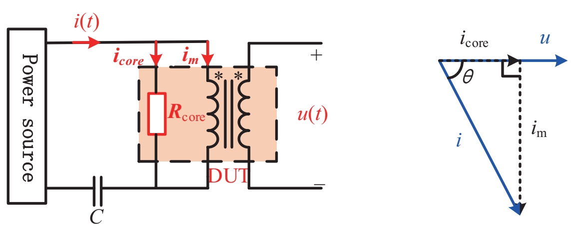

(a) (b)

Fig. 4. Schematic diagram of the measurement principle of the large-signal AC method. (a) Equivalent circuit diagram. (b) Current and voltage vector diagram.

parameters A_e, l_e, and V_e are calculated with (11), and the specimen under test is shown in Fig. 3.

$$\begin{cases} A_e = \dfrac{(OD-ID)\cdot h}{2} \\ l_e = \dfrac{\pi\cdot(OD-ID)}{\ln(OD/ID)} \\ V_e = \pi\cdot h\cdot\left[\left(\dfrac{OD}{2}\right)^2-\left(\dfrac{ID}{2}\right)^2\right] \end{cases} \tag{11}$$

The large-signal AC method is usually used to measure the AC magnetization curve and core losses under sinusoidal wave excitation. The measurement principle is shown in Fig. 4. In the figure, the capacitor C is a DC-blocking capacitor. The DUT is wound with a double-winding. A large-signal AC excitation is applied to the DUT. The induced voltage $u(t)$ of the secondary side and the exciting current $i(t)$ of the primary side of DUT are sampled. According to Faraday's law of electromagnetic induction and Ampere's circuital law, the magnetic flux density $B(t)$ and the magnetic field intensity $H(t)$ are shown in (12).

$$\begin{cases} B(t) = \dfrac{1}{N\cdot A_e}\displaystyle\int_0^t u(t)\mathrm{d}t \\ H(t) = \dfrac{N\cdot i(t)}{l_e} \end{cases} \tag{12}$$

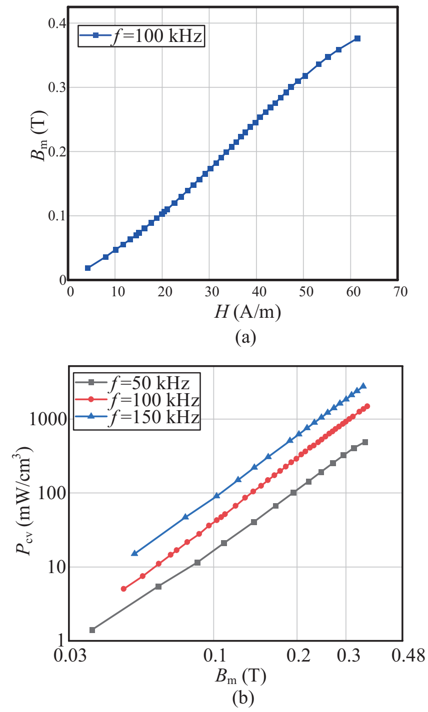

(a)

(b)

Fig. 5. Magnetic characteristic curves of ferrite (TPG33B) T22. (a) AC magnetization curve. (b) Core loss under sinusoidal wave excitation.

where A_e is the effective cross-sectional area, l_e is the effective magnetic path length, N is the winding turns, T is the period.

The hysteresis loop can be drawn according to (12). Connecting the peak points of the hysteresis loops excited by different voltages amplitudes yields the AC magnetization curve. Meanwhile, the product of the exciting current $i(t)$ and the induced voltage $u(t)$ is integrated over one period to obtain the core losses P_{core}, as shown in (13).

$$P_{core} = \frac{1}{T}\int_0^T u(t)\cdot i(t)\cdot \mathrm{d}t \tag{13}$$

The magnetization curve of the ferrite TPG33B under 100 kHz sinusoidal wave voltage excitation is shown in Fig. 5(a). The mathematical model of the magnetization curve $B_m(H)$ is shown in (14).

$$B_m(H) = B_s\cdot\frac{(H/H_0)^{\beta_2}}{1+(H/H_0)^{\beta_2}} \tag{14}$$

where B_s, H_0, and β_2 are the parameters related to the core material, and these are obtained by the least squares method as shown in Table II.

The core losses under sinusoidal wave voltages excitation whose frequency range is from 50 kHz to 150 kHz are shown in Fig. 5(b). The mathematical model of the core losses density $P_{cv}(B_m)$ is shown in (15).

$$P_{cv}(B_m) = k\cdot f^{\alpha}\cdot B_m^{\beta} \tag{15}$$

where k, α, and β are the parameters related to the core

TABLE II
MAGNETIC CHARACTERISTIC PARAMETERS OF FERRITE (TPG33B) T22

parameter	value	parameter	value
B_s	1.16653	k	0.07691
H_0	100.53436	α	1.70366
β_2	1.43403	β	2.75142

material, and these are obtained by the least squares method as shown in Table II.

III. Error Analysis of Core Losses Calculation for High-Frequency PWM Wave Excitation

There are mainly three errors of core losses calculation under PWM wave voltage excitation by using FE software Maxwell: the measurement error of magnetic characteristics of core material, the error of core losses mathematical model, and the error caused by applying different types of excitation sources.

A. The Measurement Error of Magnetic Characteristics of Core Material

The magnetic ring with a relatively small outer-to-inner diameter ratio is usually used as DUT to obtain the magnetic characteristics of core materials. It is assumed that the magnetic flux density inside the magnetic ring is uniformly distributed and is equal to the magnetic flux density at the effective magnetic path length. However, in reality, the magnetic flux density distribution inside the magnetic ring is non-uniform, which will thus lead to the magnetic characteristics measurement error of the core material.

In this paper, the T22 magnetic ring is used to obtain the magnetic characteristics of core material, and the ratio of its outer diameter to inner diameter is 1.57. If the magnetic flux density inside the magnetic ring is uniformly distributed and is equal to the magnetic flux density at the effective magnetic path length, then the magnetic field intensity H_m, magnetic flux density B_{m_ideal} inside the core and core losses P_{core_ideal} are shown in (16).

$$\begin{cases} H_m = \dfrac{N \cdot I_{pk}}{l_e} \\ B_{m\_ideal} = B_s \cdot \dfrac{(H_m / H_0)^{\beta_2}}{1+(H_m / H_0)^{\beta_2}} \\ P_{core\_ideal} = k \cdot f^{\alpha} \cdot B_{m\_ideal}^{\beta} \cdot V_e \end{cases} \tag{16}$$

where I_{pk} is the current peak value. f is exciting frequency, with a value of 100 kHz. B_s, H_0, β_2, k, α, and β are shown in TABLE II.

If the magnetic flux density distribution inside the core is non-uniform, then the core losses P_{core_Integ} is shown in (17).

$$P_{core\_Integ} = 2 \cdot \pi \cdot h \cdot k \cdot f^{\alpha} \cdot \int_{r_2}^{r_1} \left(B_s \cdot \dfrac{(\dfrac{N \cdot I_{pk}}{2 \cdot \pi \cdot r \cdot H_0})^{\beta_2}}{1+(\dfrac{N \cdot I_{pk}}{2 \cdot \pi \cdot r \cdot H_0})^{\beta_2}} \right)^{\beta} \cdot r\mathrm{d}r \tag{17}$$

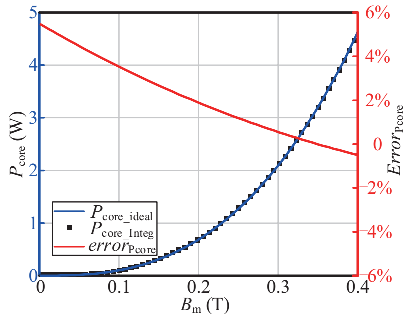

Fig. 6. Relationship diagram between core loss calculation error and magnetic flux density.

where r_1 is the outer diameter of the T22 magnetic ring, r_2 is the inner diameter of the T22 magnetic ring. Therefore, the relative error which is caused by using the T22 to measure the magnetic characteristics of core material is as shown in (18).

$$error_{P_{core}} = \frac{P_{core\_Integ} - P_{core\_ideal}}{P_{core\_Integ}} \cdot 100\% \tag{18}$$

The relative measurement error curve e is plotted according to (16), (17) and (18), as shown in Fig. 6. It can be seen from the figure that the curves of P_{core_ideal} and P_{core_Integ} coincide, and the maximum relative error between the two curves is only 5.46%. Therefore, the magnetic characteristics of core material can be accurately obtained by using the magnetic ring T22.

B. Error of the Mathematical Model for Core Losses

In the transient field solver, the instantaneous value of the core losses is obtained using the equivalent elliptical loop (EEL) model [17] which is based on the parameters k, α, and β of the SE equation, as shown in (19).

$$\begin{cases} C = \pm \dfrac{1}{C_{\alpha\beta}} k \cdot \left| B_m \cos(\theta) \right|^{\beta-\alpha} \\ C_{\alpha\beta} = (2\pi)^{\alpha} \cdot \dfrac{2}{\pi} \displaystyle\int_0^{\frac{\pi}{2}} \cos^{\beta}(\theta) \cdot \mathrm{d}\theta \\ p_{cv}(t) = \left| C \right| \cdot \left| \dfrac{\mathrm{d}B}{\mathrm{d}t} \right|^{\alpha} \end{cases} \tag{19}$$

The MSE is proposed for core losses simulation in this paper. Taking the ferrite T22 magnetic ring as the research object, the calculation errors of the two methods are analyzed. The core losses under PWM wave voltage excitation are calculated using the MSE and the EEL model respectively, and the exciting frequency is set to 100 kHz. After that, the calculation results are compared with the measured value of

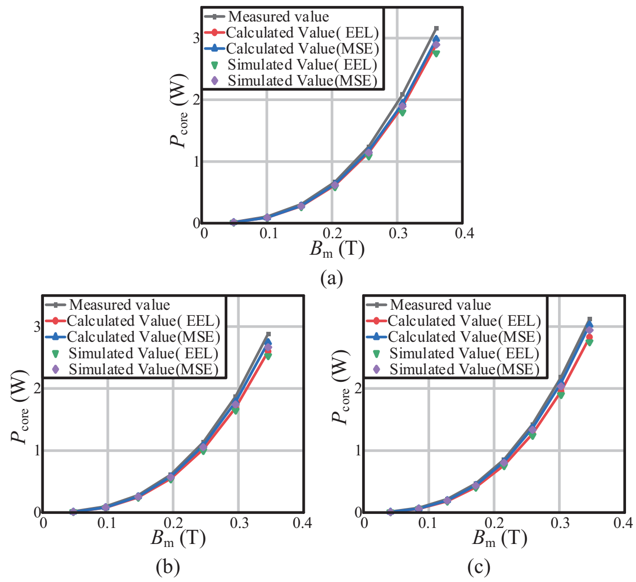

Fig. 7. Core loss of ferrite (TPG33B) T22 magnetic ring under PWM excitation at different duty cycles. (a) Duty = 0.5. (b) Duty = 0.4. (C) Duty = 0.3.

core losses, as shown in Fig. 7. It can be seen from the figure that under different duty cycles, the calculation error of core losses by using the MSE model is smaller than that of the EEL model. Therefore, the simulation scheme which is by using the MSE model is proposed to analyze the core losses under PWM wave voltage excitation in this paper.

Furthermore, the simulation results of EEL are compared with these of the proposed scheme, as shown in Fig. 7. The conclusion is consistent with the calculated conclusion. And the maximum absolute error for the magnetic ring in Fig. 7 is 0.26 W, corresponding to a relative error of 8.36%.

C. Errors of Different Excitation Types

In the FE software Maxwell, the voltage excitation can be applied to magnetic components, or the corresponding current excitation can also be applied. Due to the differences between the ways of applying the two types of excitations, the FE calculation processes of the two will result in calculation errors.

Taking the T22 magnetic ring as the research object, the error caused by different excitation types is analyzed. The core and winding of the magnetic component which is wound with T22 magnetic ring have a planar symmetric structure. Therefore, the three-dimensional model can be simplified into a two-dimensional model for simulation. Using the xoy plane as the cross-section, the simulation physical model is established in rectangular coordinate system, as shown in Fig. 8.

The transient field solver is selected. The sinusoidal voltage excitation with a frequency of 100 kHz and an amplitude of 30 V, or the sinusoidal current excitation with an amplitude of 0.31 A is applied to the magnetic component. The corresponding magnetic flux density peaks are both 0.2 T. The voltage and current waveforms on the magnetic component, as well as the instantaneous value of core losses, are shown in Fig. 9.

From Fig. 9, when the sinusoidal excitation voltage is applied to the magnetic component, the instantaneous values of the excitation current and the core losses are close to sinusoidal

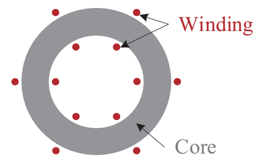

Fig. 8. Simulated physical model of ferrite (TPG33B) T22 magnetic ring.

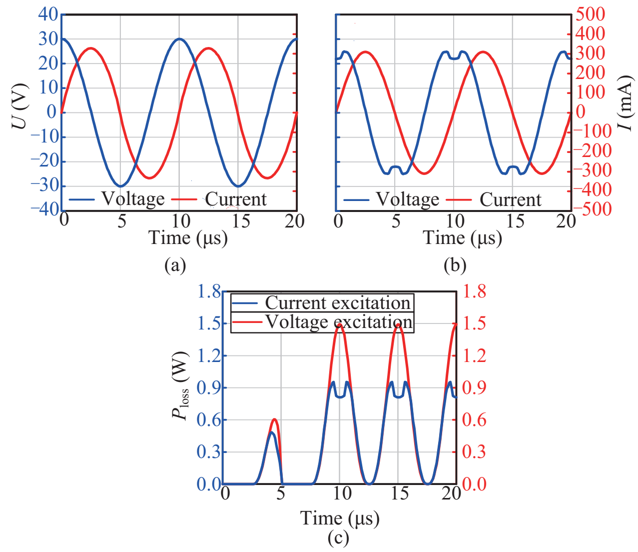

Fig. 9. Waveform diagram of excitation voltage, current and loss in transient field simulation. (a) Voltage and current of the core winding under voltage excitation. (b) Voltage and current of the core winding under current excitation. (c) Simulation diagrams of instantaneous core loss under voltage excitation or current excitation.

waves, which is consistent with the actual waveform. However, when the sinusoidal current excitation is applied to the magnetic component, there are depression phenomena at the peak of the excitation voltage and the instantaneous value of the core losses, which is inconsistent with the actual waveform. This is because the magnetic permeability of the core material has non-linear properties, resulting in differences during the FE analysis process for different excitation types.

In addition to the influence of different excitation types on the exciting waveform and core losses of magnetic ring, different excitation types also have different effects on magnetic components with air gap. When the core is of the EE type or RQ type and the magnetic component is wound by splicing two halves, there is usually an installation air gap l_g. This installation air gap is difficult to measure accurately and affects the core losses. When a voltage excitation $u(t)$ is applied to the magnetic component, the magnetic flux density $B(t)$ inside the core can be obtained with (20).

$$B(t) = \frac{\int u(t)\mathrm{d}t}{N \cdot A_e} \tag{20}$$

When a current excitation i(t) is applied to the magnetic component, the magnetomotive force and the magnetic potential drop in the air gap satisfy the ampere-turn balance, then the magnetic flux density $B(t)$ inside the core can be

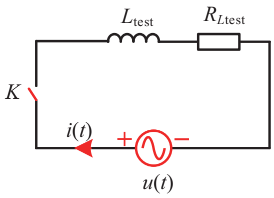

Fig. 10. Equivalent circuit diagram of the core series model.

obtained with (21).

$$B(t) = \mu_0 \cdot \frac{i(t) \cdot N}{l_g} \tag{21}$$

From (20) and (21), when the voltage excitation is applied to the magnetic component, the magnetic flux density distribution inside the core is independent of the air gap. However, when the current excitation is applied, the magnetic flux density distribution in the core is closely related to the air gap. Therefore, voltage excitation can effectively avoid the magnetic flux density distribution calculation error caused by the air gap, thereby reducing the core losses calculation error.

When a sinusoidal voltage excitation is applied to DUT, as shown in (22).

$$u(t) = U_m \cos(\omega t + \varphi_k) \tag{22}$$

where φ_k is the initial phase, and its range is from −90° to + 90°.

The R-L series equivalent circuit of the magnetic component is shown in Fig. 10. The Kirchhoff voltage circuit equation can be obtained, as shown in (23).

$$\begin{cases} L_{\text{test}} \dfrac{di}{dt} + R_{L\text{test}} \cdot i = U_m \cdot \cos(\omega t + \varphi_k) \\ \tan\varphi = \dfrac{\omega \cdot L_{\text{test}}}{R_{L\text{test}}} \end{cases} \tag{23}$$

where L_{test} is the equivalent inductance of the DUT, R_{test} is the equivalent resistance of the DUT.

The excitation current which will not experience sudden changes can be obtained with (24).

$$\begin{aligned} i = & \frac{U_m}{\sqrt{R_{L\text{test}}^2 + (\omega \cdot L_{\text{test}})^2}} \cdot \cos(\omega t + \varphi_k - \varphi) - \\ & \frac{U_m}{\sqrt{R_{L\text{test}}^2 + (\omega \cdot L_{\text{test}})^2}} \cdot \cos(\varphi_k - \varphi) \cdot e^{-\frac{t}{\tau}} \end{aligned} \tag{24}$$

where τ is time constant. When the time approaches ∞, the current becomes stable. In practice, when the time reaches 5τ (at the millisecond level), the current becomes stable. However, when the difference between φ_k and φ is 90°, there is no transient process in the circuit.

In the transient field solver of FE software Maxwell, voltage excitations with different initial phases are applied to the magnetic component (as shown in Fig. 8), and the excitation voltage and current waveforms are shown in Fig. 11. When

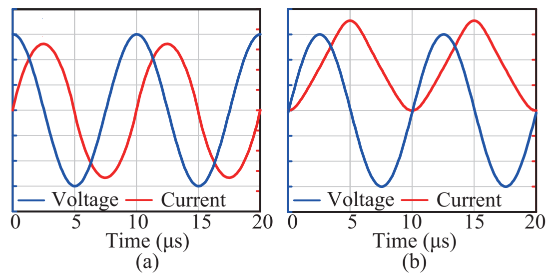

Fig. 11. Voltage and current waveforms in transient field simulation with different initial phases. (a) $\varphi_k = 0°$. (b) $\varphi_k = 90°$.

the initial phase is 0, the circuit quickly reaches a steady state; when the initial phase is 90°, there is an initial DC bias current and the current does not reach a stable state. Therefore, when the initial phase of the cosine voltage excitation is zero, the calculation time can be effectively saved.

In conclusion, when the core losses of magnetic components are calculated using the FE software Maxwell, a sinusoidal wave voltage excitation with an initial phase of zero should be applied to the magnetic components. In other words, the voltage excitation should be applied to the magnetic components, and initial state of the circuit should be zero in order that the stable state is reached in advance.

IV. Accuracy Verification of the Core Losses Simulation Scheme

In this section, the EE41 type core is taken as the research object. Based on the magnetic characteristics of the core material obtained from the ferrite T22 magnetic ring, the proposed simulation scheme for core losses is used to analyze the core losses under PWM wave voltage excitation. The simulation results are then compared with the measured values of the core losses to verify the feasibility and calculation accuracy of the scheme.

A. Core Losses Measurement Under PWM Wave Voltage Excitation

The equivalent circuit model of the magnetic component is shown in Fig. 4(a). When the large-signal AC method is utilized for core losses measurement under PWM wave voltage excitation, the waveforms of i_L, i_{core}, and i_m are shown in Fig. 12. Δt is the delay between the sampled voltage and current, and the relative measurement error δ is shown in (25).

$$\delta = \frac{\Delta P_{\text{core}}}{P_{\text{core}}} \approx \frac{I_{\text{m\_pp}} \cdot \Delta t}{D \cdot (1-D) \cdot I_{\text{core\_pp}} \cdot T} \tag{25}$$

where $I_{\text{m\_pp}}$ is the peak to peak of i_m, $I_{\text{core\_pp}}$ is the peak to peak of i_{core}, as shown in (24).

$$\begin{cases} I_{\text{m\_pp}} = \dfrac{U_{2\text{pp}} \cdot D \cdot (1-D)}{f \cdot L} \\ I_{\text{core\_pp}} = \dfrac{U_{2\text{pp}}}{R_{\text{core}}} \end{cases} \tag{26}$$

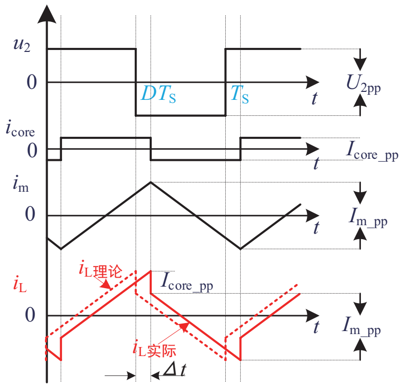

Fig. 12. Voltage and current waveforms under rectangular wave excitation.

where U_{2pp} is the peak-to-peak value of the exciting voltage.

By combining (25) and (26), the relative measurement error is shown in (27).

$$\delta = \frac{\Delta P_{core}}{P_{core}} \approx \tan\theta \cdot \Delta\theta \cdot \frac{R_{rec\_core}}{R_{sin\_core}} \tag{27}$$

where θ is the impedance angle of the magnetic component. R_{rec_core} is the equivalent resistance of the core losses under PWM wave voltage excitation. R_{sin_core} is the equivalent resistance of the core losses under sinusoidal wave voltage excitation. When the impedance angle θ is close to 90°, a tiny delay will lead to a very large measurement error. When the excitation frequency and magnetic flux density are the same, and the duty cycle is greater than 0.282 as known from (5), the measurement error of PWM voltage excitation is greater than that of sinusoidal wave excitation. In addition, the PWM wave voltage has a steep rising edge and contains high-order harmonics, so the measurement error is further increased.

Therefore, the DC power method is utilized to measure the core losses under high-frequency PWM wave excitation in this paper. The measurement principle of DC power method is shown in Fig. 13(a). The DC voltage source is converted into a PWM wave voltage through the inverter circuit and applied to the magnetic component. The magnetic component losses P_L can be obtained by subtracting the inverter circuit losses P_{ex} from the output power P_{in} of the DC voltage source, as shown in (28).

$$\begin{cases} P_L = P_{in} - P_{ex} \\ P_{in} = U_{in} \cdot I_{in} \end{cases} \tag{28}$$

where I_{in} is the DC component of the input current i_{in}, U_{in} is the input voltage.

A multimeter is only utilized to measure the DC components of the input voltage and input current to obtain the magnetic component losses by the DC power method. It avoids the problem that the measurement accuracy of the large-signal AC method is sensitive to delay errors. In [14], based on the optimized design to minimize the inverter circuit losses P_{ex}, the air-core inductor is utilized to calibrate P_{ex} to improve the

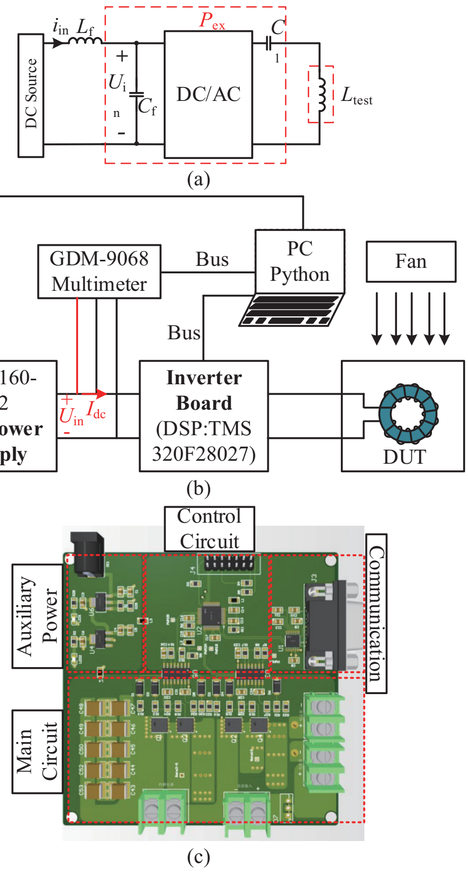

Fig. 13. DC power method measurement system. (a) DC power method measurement schematic diagram. (b) System diagram. (c) The inverter board's PCB layout (top view).

measurement accuracy of the DC power method. [18] proposes a separation scheme for core losses and winding loss of PWM wave excitation based on the DC power method. The system diagram and the inverter board's PCB layout (top view) of the DC power method are shown in Fig. 13(b) and (c).

B. Verification of the Simulation Accuracy of Core losses Under PWM Wave Voltage Excitation

The dimensions of the EE41 core and the wound specimen are shown in Fig. 14(a). The EE-type core has structural symmetry, so the three-dimensional model can be simplified to a two-dimensional model for simulation. The established two-dimensional simulation physical model is shown in Fig. 14 (b). The Polyline in the figure is a line drawn for analyzing the magnetic flux density inside the core.

The PWM wave voltage excitation (with a frequency of 100 kHz, a duty cycle of 0.5, and voltage amplitudes of 30 V and 70 V respectively) is applied to the magnetic component. The distribution of its magnetic flux density peak is shown in Fig. 15. The distribution of the magnetic flux density in the EE-shaped core is uneven, with relatively large magnetic flux density at the inner corners of the magnetic column and relatively small magnetic flux density at the outer corners. The span of the magnetic flux density distribution and the core losses density of the EE-shaped core is wide.

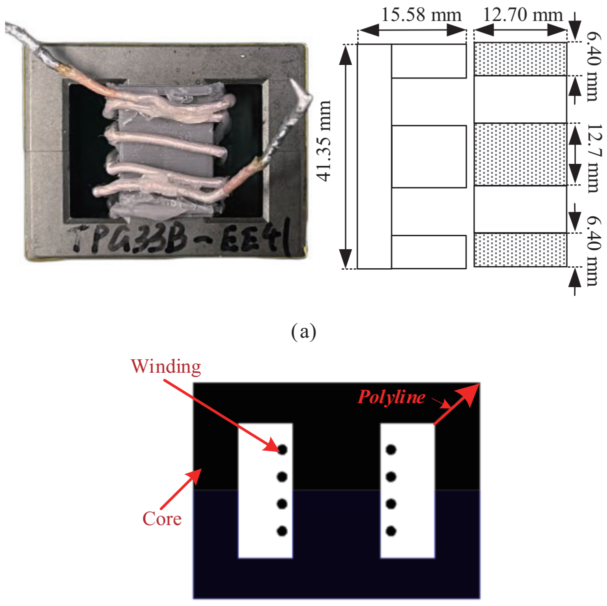

Fig. 14. Parameters of ferrite (TPG33B) EE-shaped core. (a) Dimensions of ferrite (TPG33B) EE-shaped core. (b) Two-dimensional simulation model of ferrite (TPG33B) EE-shaped core.

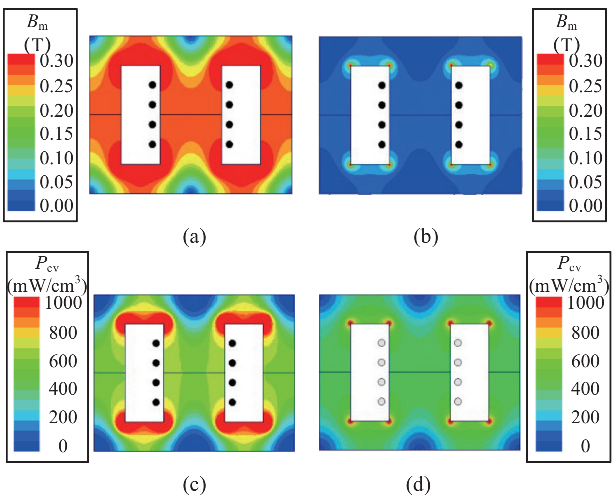

Fig. 15. Field distribution diagram of ferrite (TPG33B) EE core. (a) Peak distribution of magnetic flux density (excitation voltage: 70 V). (b) Peak distribution of magnetic flux density (excitation voltage: 30 V). (c) Distribution of core loss density (excitation voltage: 70 V). (d) Distribution of core loss density (excitation voltage: 30 V).

The distribution of the magnetic flux density peak on the Polyline is shown in Fig. 16. The span of the distribution of the magnetic flux density peak is from 0 T to 0.5 T, and its distribution is complex. A comparison between the simulation results and measurements of the core losses of the EE-shaped core is shown in Fig. 17. The abscissa in the figure represents the amplitude of the excitation voltage. It can be seen from the figure that the simulation results and measurements of the core losses at different duty cycles are basically in agreement. When the amplitude of the excitation voltage is relatively large, the absolute error is relatively large. This is because the

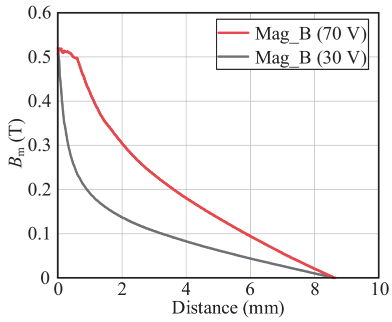

Fig. 16. Peak distribution of magnetic flux density along the Polyline of the Ferrite (TPG33B) EE core.

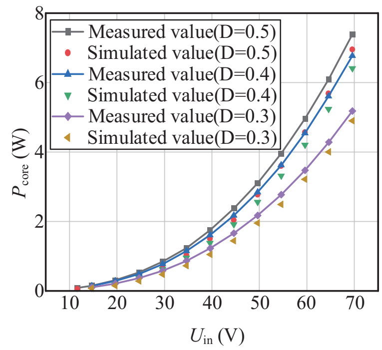

Fig. 17. Core loss diagram of ferrite (TPG33B) EE core under PWM excitation.

distribution range of the magnetic flux density is too wide, and the mathematical model of the core losses density for a wide range of magnetic flux densities needs to be further improved.

V. Conclusion

By using FE software Ansys Maxwell, this paper proposes a simulation scheme for core losses calculation of magnetic components with different core structures in power converters. The core losses model under PWM wave voltage excitation is derived based on MSE, and it is equal to the core losses under sinusoidal wave voltage excitation multiplied by a coefficient which relates to duty cycle and the SE coefficient α. Therefore, based on the core losses under sinusoidal wave voltage excitation, either the transient field solver or the eddy current field solver of FE software Ansys Maxwell can be selected for core losses simulation.

The magnetic properties of core material serve as basis for accurate core losses simulation. The large-signal AC method is used for magnetic properties measurement of core materials under sinusoidal wave voltage excitation. The measurement and modeling of AC magnetization curves and core losses of ferrite (TPG33B) are obtained with magnetic ring T22. Furthermore, the main simulation error sources are analyzed. The magnetic property measurement error is due to the uneven distribution of magnetic flux density inside the magnetic ring. An accurate core losses model ensures the accuracy of core losses simulation. For the core losses of PWM wave voltage excitation, the EEL model which is the software's built-in core losses model has poorer accuracy than MSE. The FE calculation processes of different excitation types will result in calculation errors. The voltage excitation with an initial phase of zero, when initial value of the exciting current is zero, should be applied to the magnetic components.

The large-signal AC method which is used for core losses measurement under PWM wave excitation is widely inaccurate. Therefore, the core losses simulation results are compared with measurement results with DC power method, and the comparison results validated the practicability and accuracy of the proposed simulation method. The maximum absolute error for the EE-shaped magnetic core is only 0.428 W, corresponding to a relative error of 5.79%.

However, the span of magnetic flux density distribution in non-ring core is a wide range (several mT to saturation magnetic flux density), and the core losses model of wide range magnetic flux density should be further improved.

References

[1] T. Wang, R. Luo, J. Wen, M. Zhang, and J. Tian, "A measurement method of winding loss for high-frequency transformer based on auxiliary winding," in *Transactions of China Electrotechnical Society,* vol. 37, no. 10, pp. 2622–2630, May 2022.

[2] C. Peng, G. Chen, B. Wang, and J. Song, "Semi-analytical AC resistance prediction model for Litz wire winding in high-frequency transformer," in *IEEE Transactions on Power Electronics*, vol. 38, no. 10, pp. 12730–12742, Oct. 2023.

[3] S. Zhang, W. Sun, T. Fan, X. Wen, and D. Zhang, "Research on high power density silicon carbide motor controller based on parallel connection of discrete devices," in *Transactions of China Electrotechnical Society*, vol. 38, no. 22, pp. 5999–6014, Nov. 2023.

[4] X. Huang, Y. Lei, Y. Zhou, W. Du, and J. Zhang, "An ultra-high efficiency high power density 140W PD3.1 AC-DC adapter using GaN power ICs," in *2023 IEEE Applied Power Electronics Conference and Exposition (APEC)*, Orlando, FL, USA, 2023, pp. 1252–1258.

[5] L. Yi and J. Moon, "Accurately disentangling core and winding losses in experimental, in-situ magnetic loss measurement for power electronic circuits and applications," in *IEEE Journal of Emerging and Selected Topics in Power Electronics*, vol. 12, no. 6, pp. 5568–5578, Dec. 2024.

[6] A. Huang, X. Wang, H. Zhang, C. Hwang, D. Pommerenke, and J. Fan, "Improved current shunt characterization method for core loss measurement," in *IEEE Transactions on Power Electronics*, vol. 37, no. 7, pp. 8290–8300, Jul. 2022.

[7] G. Bertotti, "General properties of power losses in soft ferromagnetic materials," in *IEEE Transactions on Magnetics*, vol. 24, no. 1, pp. 621–630, Jan. 1988.

[8] N. Zhang, L. Li, and X. Wei, "Calculation method and experimental verification of core losses under non-sinusoidal excitation," in *Transactions of China Electrotechnical Society*, vol. 31, no. 17, pp. 224–232, Sept. 2016.

[9] Z. Zhao, Q. Lin, J. Ji, and X. Ma, "Wideband loss separation models of ferromagnetic materials considering skin effect," in *Proceedings of the Chinese Society of Electrical Engineering*, vol. 42, no. 14, pp. 5374–5382, Jul. 2022.

[10] J. H. Wang and W. Chen, "Study of calorimetric method to measure loss of super low loss angle core," in *Advanced Technology of Electrical Engineering and Energy*, vol. 31, no. 4, pp. 6–9, Apr. 2012.

[11] J. Wang, P. Fan, S. Lin, F. Huang, and W. Chen, "Comparative calorimetric method for magnetic component losses measurement with high frequency," in *IEEE Journal of Emerging and Selected Topics in Power Electronics*, vol. 12, no. 5, pp. 5112–5122, Oct. 2024.

[12] M. Mu, Q. Li, D. J. Gilham, F. C. Lee, and K. D. T. Ngo, "New core loss measurement method for high-frequency magnetic materials," in *IEEE Transactions on Power Electronics*, vol. 29, no. 8, pp. 4374–4381, Aug. 2014.

[13] D. Hou, M. Mu, F. C. Lee, and Q. Li, "New high-frequency core loss measurement method with partial cancellation concept," in *IEEE Transactions on Power Electronics*, vol. 32, no. 4, pp. 2987–2994, Apr. 2017.

[14] B. Liu, W. Chen, J. Wang, and Q. Chen, "A practical inductor loss testing scheme and device with high frequency pulsewidth modulation excitations," in *IEEE Transactions on Industrial Electronics*, vol. 68, no. 5, pp. 4457–4467, May 2021.

[15] J. Ye and W. Chen, "The method and device based on the differential power for measurement of high-frequency core losses," in *Proceedings of the Chinese Society of Electrical Engineering*, vol. 37, no. 16, pp. 4834–4841, Aug. 2017.

[16] J. Reinert, A. Brockmeyer, and R. W. De Doncker, "Calculation of losses in ferro- and ferrimagnetic materials based on the modified Steinmetz equation," in *Conference Record of the 1999 IEEE Industry Applications Conference. Thirty-Forth IAS Annual Meeting*, Phoenix, AZ, USA, 1999, pp. 2087–2092.

[17] D. Lin, P. Zhou, W. N. Fu, Z. Badics, and Z. J. Cendes, "A dynamic core loss model for soft ferromagnetic and power ferrite materials in transient finite element analysis," in *IEEE Transactions on Magnetics*, vol. 40, no. 2, pp. 1318–1321, Mar. 2004.

[18] D. Yang, B. Wang, S. Shao, and J. Zhang, "A novel DC differential method for high frequency core loss measurement," in *IEEE Transactions on Power Electronics*, vol. 39, no. 10, pp. 13459–13470, Oct. 2024.

Zhikang Fu was born in Jiangxi, China, in 1999. He is currently pursuing the master's degree with the Fuzhou University, Fuzhou. His research interest includes high frequency magnetic technology, engineering electromagnetic field analysis and application, etc.

Jinghui Wang was born in Jiangxi, China. She received the B.E., M.S., and Ph.D. degrees in electrical engineering from Fuzhou University, Fuzhou, China, in 1997, 2000, and 2012, respectively. She is currently an Associate Professor at Fuzhou University. Her main research interests include power electronic high frequency magnetic technology and electromagnetic characteristic measurement and model study of magnetic elements.

Juntao Xiao was born in Jiangxi, China, in 1997. He obtained her master's degree from Fuzhou University in 2023. His research interest includes magnetic component design, magnetic core loss testing technology, etc.

Wei Chen (Fellow, CPSS) was born in Jiangxi, China. He received the M.S. and Ph.D degrees in electrical engineering from Fuzhou University, Fuzhou, China, in 1987 and 1990, espectively. He worked as a Senior Visiting Professor with Center for Power Electronics Systems (CPES) of Virginia Tech, Blacksburg, VA, USA, from 1996 to 1998. His research interests include power conversion, high-frequency magnetic technology, EMI debug and solution, wireless power transfer, electromagnetic field analysis, and applications, etc.